Simulation of cross-correlated turbulence-induced phase fluctuations produced by many stars

V. V. Voitsekhovich [1], D. Kouznetsov [2]

[1] Instituto de Astronomia, UNAM. AP 70-264 Cd. Universitaria, 04510 Mexico D.F., Mexico.
[2] Centro de Instrumentos, UNAM. AP 70-186 Cd. Universitaria, 04510 Mexico D.F., Mexico.

Abstract

The modification of the method of random wave vectors (RWV) [1] allowing for a simulation of cross-correlated turbulence-induced phase fluctuations to be produced by many stars is proposed. It turns out that for the case of weak-turbulence conditions which are of importance for many applications, it is possible to suggest a relatively simple and fast procedure of simulation. The variation of C_n^2 along a propagation path and an effect of finite outer scale of the turbulence are included into consideration. The validity of the simulation is verified by comparison of theoretical and simulated results, and it is shown that a good agreement takes place even for big separations between the observation points. Adaptive optics, speckle interferometry, guide stars, imaging through the turbulence, long-base interferometry as well as simulations of the image distortions of extended objects are among the possible applications of the method developed.

1 Introduction

It has been described in the previous paper [2] how the method of random wave vectors (RWV) can be used in simulations of anisoplanatic effects associated with two stars. For the case of two stars, the approach suggested in that paper is general, i.e. it can be applied for arbitrary spectra and cross-spectrum of phase fluctuations. Unfortunately, if one needs to consider more than two stars, a complexity of its application grows and an efficiency of simulation becomes worse with the increase of the number of stars. However, for the case of the weak-turbulence conditions, it is possible to develop another modification of the RWV which allows for a relatively simple and rapid simulation of cross-correlated turbulence-induced phase fluctuations to be produced by many stars. This modification is based on a specific choice of the probability distribution for some simulation parameters that gives one a possibility to reproduce simultaneously all the correlation and cross-correlation functions associated with as many stars as one needs to consider. Since under the weak-turbulence conditions the phase fluctuations are Gaussian, the reproduction mentioned above is sufficient to provide all the needed statistics and cross-statistics in simulated samples.

Both the constant and the varying refractive-index structure characteristic as well as an effect of finite outer scale are included. The validity of the simulation is verified by comparison of the theoretical and simulated results, and it is shown that a good agreement takes place even for big separations between the observation points. Adaptive optics, speckle interferometry, guide stars, imaging through the turbulence, long-base interferometry and simulations of the image distortions of extended objects are among the possible applications of the method developed.

2 Theoretical correlations and cross-correlations.

Let us consider N stars and assume that these stars produce N monohromatic, initially plane waves at the upper boundary of the atmosphere. Then, let S_l be the phase fluctuation produced by the l-th wave at the aperture. In order to apply the RWV method, we need to calculate the correlation $B_{S_l S_l}$ $(l = 1, ..., N)$ and cross-correlation functions $B_{S_l S_j}$ $(l = 1, ..., N; j = 1, ..., N)$ associated with the fluctuations produced by all the stars. Let us introduce the three-dimensional Cartesian coordinate system with the X and Y axes placed at the aperture plane, and let $\boldsymbol{\xi}_l$ be the propagation unit vector of l-th wave at the upper boundary of the atmosphere. Applying the same development as in Ref. 2, we can express $B_{S_l S_l}$ and $B_{S_l S_j}$

$$B_{S_l S_l}(\rho) = 4\pi^2 k^2 \int_0^L \mathrm{d}z \int \mathrm{d}\kappa\kappa\Phi_n(z,\kappa)\, J_0(\kappa\rho)\,,\ l = 1, ..., N, \tag{1}$$

$$B_{S_l S_j}(\boldsymbol{\rho}) = \langle S_l(\mathbf{r_1})\, S_j(\mathbf{r_2})\rangle = 4\pi^2 k^2 \int_0^L \mathrm{d}z \int \mathrm{d}\kappa\kappa\Phi_n(z,\kappa)\, J_0(\kappa\,|\boldsymbol{\rho} - (\mathbf{n}_l - \mathbf{n}_j)\, z|)\,, \quad l = 1, ..., N;\ j = 1, ..., N, \tag{2}$$

where $\mathbf{r_1}$ and $\mathbf{r_2}$ denote the two-dimensional vectors at the aperture, $\boldsymbol{\rho} = \mathbf{r_1} - \mathbf{r_2}$, $\langle \cdots \rangle$ denotes the statistical average, k is the wavenumber, Φ_n is the isotropic spectrum of refractive-index fluctuations, ρ and κ denote the modules of the corresponding vectors, J_0 is the Bessel function, and $\mathbf{n}_l$ is the projection of the propagation vector $\boldsymbol{\xi}_l$ on the aperture plane. In derivation of Eqs. (1, 2) we have used the approximation $1 + \cos\left(\frac{\kappa^2 z}{k}\right) \approx 2$ that holds with a good accuracy in problems related to the light propagation through the atmospheric turbulence [3].

In what follows we use the von Karmann refractive-index spectrum Φ_n [4] :

$$\Phi_n(z,\kappa) = 0.033 C_n^2(z)\left(\kappa^2 + 1/L_0^2\right)^{-11/6}, \tag{3}$$

where $C_n^2(z)$ is the profile of the refractive-index structure characteristic, and L_0 denotes the outer scale of the turbulence.

Substituting Eq. (3) into Eqs. (1, 2) we have

$$B_{S_l S_l}(\rho) = 0.132\pi^2 k^2 \int_0^L \mathrm{d}z C_n^2(z) \int_0^\infty \mathrm{d}\kappa\kappa\left(\kappa^2 + 1/L_0^2\right)^{-11/6} J_0(\kappa\rho)\,,\ l = 1, ..., N, \tag{4}$$

$$B_{S_l S_j}(\boldsymbol{\rho}) = 0.132\pi^2 k^2 \int_0^L \mathrm{d}z C_n^2(z) \int_0^\infty \mathrm{d}\kappa\kappa\,(\kappa^2 + 1/L_0^2)^{-11/6}\, J_0(\kappa\,|\boldsymbol{\rho} - (\mathbf{n}_l - \mathbf{n}_j)\, z|)\,, \quad l = 1, ..., N;\ j = 1, ..., N. \tag{5}$$

Introducing the two-dimensional spectrum $W(\boldsymbol{\kappa})$ of the function $B(\boldsymbol{\rho})$ as:

$$W(\boldsymbol{\kappa}) = \frac{1}{2\pi} \int \mathrm{d}^2\rho \; B(\boldsymbol{\rho}) \exp(i\boldsymbol{\kappa} \cdot \boldsymbol{\rho}), \tag{6}$$

and applying the transformation (6) to Eqs. (4, 5), we get the following expressions for the spectra $W_{S_l S_l}$ and for the cross-spectra $W_{S_l S_j}$ of phase fluctuations

$$W_{S_l S_l}(\kappa) = 0.132\pi^2 k^2 \left(\kappa^2 + 1/L_0^2\right)^{-11/6} \int_0^L \mathrm{d}z C_n^2(z), \; l = 1, ..., N, \tag{7}$$

$$\begin{aligned} &\mathrm{Re}\, W_{S_l S_j}(\boldsymbol{\kappa}) = 0.132\pi^2 k^2 (\kappa^2 + 1/L_0^2)^{-11/6} \int_0^L \mathrm{d}z C_n^2(z) \cos\left[\boldsymbol{\kappa} \cdot (\mathbf{n}_l - \mathbf{n}_j) z\right], \\ &\mathrm{Im}\, W_{S_l S_j}(\boldsymbol{\kappa}) = 0.132\pi^2 k^2 (\kappa^2 + 1/L_0^2)^{-11/6} \int_0^L \mathrm{d}z C_n^2(z) \sin\left[\boldsymbol{\kappa} \cdot (\mathbf{n}_l - \mathbf{n}_j) z\right], \\ &l = 1, ..., N; \; j = 1, ..., N, \end{aligned} \tag{8}$$

where Re and Im denote the real and the imaginary parts of complex quantity.

3 Simulation method: theoretical derivations

We need to simulate the phase fluctuations $S_l(\mathbf{r})$ in such a way that all the simulated correlation functions $B^e_{S_l S_l}$ $(l = 1, ..., N)$ and the cross-correlation functions $B^e_{S_l S_j}$ $(l = 1, ..., N; j = 1, ..., N)$ coincide with the corresponding theoretical ones. As it will be seen below, the conditions above are satisfied if the phase fluctuations at the observation plane are simulated as

$$S_l(\mathbf{r}) = \sum_{m=1}^{M} F(p_m) \cos(\mathbf{p}_m \cdot \mathbf{r} + \varphi_m - \mathbf{p}_m \cdot \mathbf{n}_l \psi_m), \; l = 1, ..., N. \tag{9}$$

In what follows the modules p_m and the orientations θ_m of the vectors $\mathbf{p}_m$, and the phases φ_m and ψ_m are considered as statistically independent quantities. As it will be seen below, the ψ_m have the dimension of the length. By definition, θ_m and φ_m are distributed uniformly inside the range $[-\pi, \pi]$.

We choose the probability density function (PDF) $\eta(\psi_m)$ of ψ_m and the magnitudes $F(p_m)$ in such a way that the theoretical correlation and cross-correlation functions (4, 5) coincide with the corresponding functions following from (9).

Using the same development as in Ref. 1, one can write a condition of coincidence as

$$B_{S_l S_l}(\rho) = \tfrac{1}{2} \sum_{m=1}^{M} \left\langle F^2(p_m) \cos(\mathbf{p}_m \cdot \boldsymbol{\rho}) \right\rangle, \; l = 1, ..., N, \tag{10}$$

$$B_{S_l S_j}(\boldsymbol{\rho}) = \tfrac{1}{2} \sum_{m=1}^{M} \left\langle F^2(p_m) \cos[\mathbf{p}_m \cdot \boldsymbol{\rho} - \mathbf{p}_m \cdot (\mathbf{n}_l - \mathbf{n}_j) \psi_m] \right\rangle, \; l = 1, ..., N; j = 1, ..., N. \tag{11}$$

Applying the transformation (6) to Eqs. (10, 11), we get

$$W_{S_l S_l}(\kappa) = \tfrac{\pi}{2} \sum_{m=1}^{M} \int \mathrm{d}^2 p_m \; F^2(p_m) \Omega(\mathbf{p}_m) \left[\delta(\mathbf{p}_m + \boldsymbol{\kappa}) + \delta(\mathbf{p}_m - \boldsymbol{\kappa})\right], \; l = 1, ..., N, \tag{12}$$

$$W_{S_l S_j}(\boldsymbol{\kappa}) = \frac{\pi}{2} \sum_{m=1}^{M} \int \mathrm{d}\psi_m \, \eta(\psi_m) \int \mathrm{d}^2 p_m F^2(p_m) \, \Omega(\mathbf{p}_m) \times$$
$$\{\exp[-i\mathbf{p}_m \cdot (\mathbf{n}_l - \mathbf{n}_j)\psi_m] \, \delta(\mathbf{p}_m + \boldsymbol{\kappa}) + \exp[i\mathbf{p}_m \cdot (\mathbf{n}_l - \mathbf{n}_j)\psi_m] \, \delta(\mathbf{p}_m - \boldsymbol{\kappa})\}, \quad (13)$$
$$l = 1, ..., N; j = 1, ..., N,$$

where Ω and η are the PDF's of the vector $\mathbf{p}_m$ and ψ_m, respectively.

Since the processes under simulation are isotropic, the PDF Ω can also be chosen as an isotropic function, i.e. $\Omega(\boldsymbol{\kappa}) = \Omega(\kappa)$. Performing the integration over p_m and the summation over m in Eq. (12), we get the $F(\kappa)$ as

$$F(\kappa) = \sqrt{\frac{W_{S_l S_l}(\kappa)}{\pi M \Omega(\kappa)}}, \; l = 1, ..., N. \quad (14)$$

Performing the same operations in Eq. (13), and taking into account Eqs. (7, 8, 14), one can get the following relationship between the PDF of ψ_m and C_n^2 profile

$$\int \mathrm{d}\psi_m \, \eta(\psi_m) \cos[\boldsymbol{\kappa} \cdot (\mathbf{n}_l - \mathbf{n}_j)\psi_m] = \int_0^L \mathrm{d}z C_n^2(z) \cos[\boldsymbol{\kappa} \cdot (\mathbf{n}_l - \mathbf{n}_j) z] \Big/ \int_0^L \mathrm{d}z C_n^2(z),$$
$$\int \mathrm{d}\psi_m \, \eta(\psi_m) \sin[\boldsymbol{\kappa} \cdot (\mathbf{n}_l - \mathbf{n}_j)\psi_m] = \int_0^L \mathrm{d}z C_n^2(z) \sin[\boldsymbol{\kappa} \cdot (\mathbf{n}_l - \mathbf{n}_j) z] \Big/ \int_0^L \mathrm{d}z C_n^2(z), \quad (15)$$
$$l = 1, ..., N; j = 1, ..., N.$$

Since $C_n^2(z)$ is a non-negative function, we can always choose the PDF of ψ_m in such a way that Eq. (15) will be satisfied for all the l and j. The needed PDF is given by

$$\eta(\psi_m) = \left\{ \begin{array}{l} C_n^2(\psi_m) \Big/ \int_0^L \mathrm{d}z C_n^2(z), \; 0 \le \psi_m \le L \\ 0, \; \text{otherwise.} \end{array} \right\} \quad (16)$$

As one can see, the PDF (16) forces both equations (15) to be the identities. From the practical point of view it means that if $F(\kappa)$ and $\eta(\psi_m)$ are determined from Eqs. (14, 16), respectively, the simulation with Eq. (9) provides all the necessary correlations and cross-correlations among the simulated phase fluctuations. The PDF (16) can be generated for an arbitrary C_n^2 profile using, for example, the rejection method [5].

Let us choose now the PDF $\Omega(\kappa)$. Since all the processes have the same spectra (7), we can seek the PDF $\Omega_\kappa(\kappa)$ of the module of vector $\boldsymbol{\kappa}$ matching to these spectra. Basing on the above consideration, we choose the Lorentzian PDF [5] as follows:

$$\Omega_\kappa(\kappa) = \frac{1}{\Omega_0 (\kappa^2 + 1/L_0^2)}, \; \Omega_0 = L_0 [\arctan(K_2 L_0) - \arctan(K_1 L_0)], \quad (17)$$

where K_1 and K_2 are the lower and the upper boundaries of the region of spacial frequencies inside which the phase fluctuations are simulated. By definition, the PDF $\Omega_\kappa(\kappa)$ is considered to be equal to zero outside the above region.

The corresponding PDF $\Omega(\kappa)$ of the vector $\boldsymbol{\kappa}$ is given by

$$\Omega(\kappa) = \frac{1}{2\pi\Omega_0 \kappa (\kappa^2 + 1/L_0^2)}. \quad (18)$$

Making use of the considerations above, the samples S_l are simulated as follows.

1. The set $\{s_m\}$ of M random numbers s_m distributed uniformly inside the range $[0, 1]$ is generated. Then, in order to get the set of $\{p_m\}$ distributed with the PDF (17), the following transformation is applied:

$$p_m = \frac{1}{L_0} \tan\left\{s_m L_0 \left[\arctan\left(K_2 L_0\right) - \arctan\left(K_1 L_0\right)\right]\right\}. \tag{19}$$

Generating M random, uniformly distributed inside the range $[-\pi, \pi]$ angles θ_m, we obtain M random vectors $\mathbf{p}_m$ with PDF given by Eq. (18).

2. Making use of the sets $\{p_m\}$ and $\{\theta_m\}$ simulated at the step 1, we calculate the magnitudes of $W_{S_l S_l}\left(p_m\right)$ and $\Omega\left(p_m\right)$. Since, as it follows from (7), the $W_{S_l S_l}$ do not depend on l, the magnitude of $W_{S_l S_l}\left(p_m\right)$ is calculated only one time. Substituting $W_{S_l S_l}\left(p_m\right)$ and $\Omega\left(p_m\right)$ into Eq. (14), we get the amplitudes $F\left(p_m\right)$.

3. M random magnitudes of ψ_m distributed with PDF (16) are generated for given C_n^2 profile.

4. M random, uniformly distributed inside the range $[-\pi, \pi]$ magnitudes of φ_m are generated.

5. Substituting the sets of $\{F\left(p_m\right)\}, \{\mathbf{p}_m\}, \{\varphi_m\}$, and $\{\psi_m\}$ into Eq. (9), the samples $S_l\left(\mathbf{r}\right)$ $(l = 1, ..., L)$ can be calculated at any chosen grid of coordinates $\mathbf{r}$.

Note, that there is no necessity to calculate the cross-spectra $W_{S_l S_j}\left(p_m\right)$ in the simulation because all the needed cross-correlations are provided by the special choice (16) of the PDF of ψ_m. This is an additional advantage of the PDF (16) allowing to accelerate significantly the simulation.

In some applications the simulation of the total wave field $U\left(\mathbf{r}\right)$ to be produced by N stars is of interest. Since under the weak-turbulence conditions the influence of amplitude fluctuations is practically negligible [6], the samples of $U\left(\mathbf{r}\right)$ can be simulated through the samples of phase fluctuations S_l as follows

$$U\left(\mathbf{r}\right) = \sum_{l=1}^{N} A_l \exp\left[iS_l\left(\mathbf{r}\right) + i\kappa \mathbf{r} \cdot \mathbf{n}_l\right], \tag{20}$$

where A_l is the amplitude of l-th wave.

4 Simulation results

To demonstrate the efficiency of the approach developed for the many-stars case, it is sufficient to consider the case of three stars. In this case the cross-correlation functions which have to be reproduced in simulation are: $B_{S_1 S_1}, B_{S_1 S_2}, B_{S_1 S_3}$ and $B_{S_2 S_3}$. We compare below the simulated and theoretical cross-correlation functions of interest for both a constant C_n^2 along the propagation path (horizontal path) and for a varying C_n^2 as well. For both cases the simulation parameters have been chosen as follows: the number of harmonics $M = 100$, the frequency limits: $K_1 = 0$, $K_2 = 10^4$ 1/m .

4.1 Horizontal path

If the propagation along a horizontal path is of interest, $C_n^2\left(z\right)$ is a constant, i.e. $C_n^2\left(z\right) = C_n^2$, and the formulas for the correlation and cross-correlation functions and for the corresponding spectra

and cross-spectra are reduced to

$$
\begin{aligned}
B_{S_l S_l}(\rho) &= 0.132\pi^2 k^2 C_n^2 Z \int_0^\infty \mathrm{d}\kappa\kappa \left(\kappa^2 + 1/L_0^2\right)^{-11/6} J_0(\kappa\rho), \\
B_{S_l S_j}(\boldsymbol{\rho}) &= 0.132\pi^2 k^2 C_n^2 \int_0^L \mathrm{d}z \int_0^\infty \mathrm{d}\kappa\kappa \left(\kappa^2 + 1/L_0^2\right)^{-11/6} J_0\left(\kappa \left|\boldsymbol{\rho} - (\mathbf{n}_l - \mathbf{n}_j)\, z\right|\right),
\end{aligned}
\tag{21}
$$

$$
\begin{aligned}
W_{S_l S_l}(\kappa) &= 0.132\pi^2 k^2 \left(\kappa^2 + 1/L_0^2\right)^{-11/6} C_n^2 L, \\
\mathrm{Re}\, W_{S_l S_j}(\boldsymbol{\kappa}) &= 0.132\pi^2 k^2 \left(\kappa^2 + 1/L_0^2\right)^{-11/6} C_n^2 L \frac{\sin\left[\boldsymbol{\kappa}\cdot(\mathbf{n}_l - \mathbf{n}_j)\, L\right]}{\boldsymbol{\kappa}\cdot(\mathbf{n}_l - \mathbf{n}_j)\, L}, \\
\mathrm{Im}\, W_{S_l S_j}(\boldsymbol{\kappa}) &= 0.132\pi^2 k^2 \left(\kappa^2 + 1/L_0^2\right)^{-11/6} C_n^2 L \frac{1 - \cos\left[\boldsymbol{\kappa}\cdot(\mathbf{n}_l - \mathbf{n}_j)\, L\right]}{\boldsymbol{\kappa}\cdot(\mathbf{n}_l - \mathbf{n}_j)\, L}.
\end{aligned}
\tag{22}
$$

Despite of, as it has been mentioned above, the cross-spectra are not used directly in the simulation, we present the corresponding formulas for the reference.

As it follows from Eq. (16), the ψ_m are distributed uniformly inside the range $[0, L]$, i.e. the PDF $\eta(\psi_m)$ is given by

$$
\eta(\psi_m) = \left\{ \begin{array}{l} 1/L,\ 0 \le \psi_m \le L \\ 0,\ \text{otherwise.} \end{array} \right\}
\tag{23}
$$

As an example, the theoretical and simulated cross-correlation functions are compared in Fig. 1 for the case of three stars. One can see that the simulation reproduces with a good accuracy all the correlations among the associated phase fluctuations.

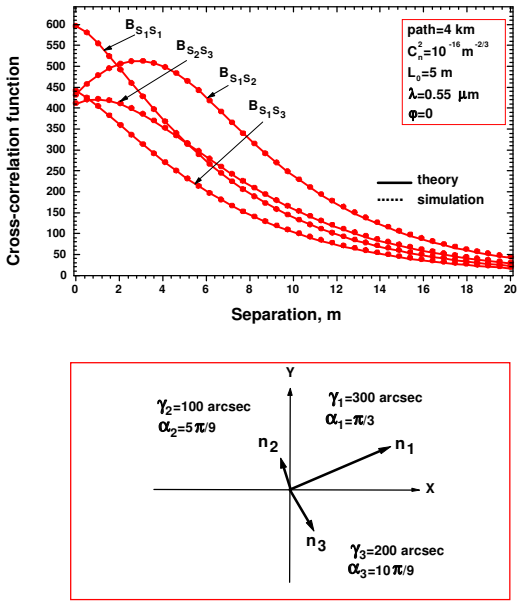

Fig. 1. Theoretical and simulated cross-correlation functions: constant C_n^2 along the path. The cross-correlation functions are anisotropic but homogeneous, i. e. they can be presented as functions of two scalar arguments: the separation $\rho = |\mathbf{r}_1 - \mathbf{r}_2|$ between two observation points $\mathbf{r}_1$ and $\mathbf{r}_2$, and the polar angle φ of the vector $\mathbf{r}_1 - \mathbf{r}_2$. The angle φ is chosen as a parameter in the top graph. The bottom graph shows thematically the alignment of stars. $\mathbf{n}_l$ is the projection of l-th propagation vector on the aperture plane, γ_l is the angular separation between l-th star and Z-axis, α_l is the polar angle of the vector $\mathbf{n}_l$.

4.2 C_n^2 varying along the path

As an example of simulation with a varying C_n^2, we present the simulation results with the Hufnagel C_n^2 profile [7]:

$$C_n^2(z) = C_0\, r_0^{-5/3} k^{-2} \left[\left(\frac{z}{z_0} \right)^{10} \exp\left\{ -\frac{z}{z_1} \right\} + \exp\left\{ -\frac{z}{z_2} \right\} \right], \tag{24}$$

where r_0 is the Fried parameter, $C_0 = 1.027 \times 10^{-3}$ m^{-1}, $z_0 = 4.632 \times 10^3$ m, $z_1 = 10^3$ m, $z_2 = 1.5 \times 10^3$ m.

In Eq. (24), the altitude z and the Fried parameter r_0 are given in meters, the wavenumber k is given in inverse meters, and the units of C_n^2 are meters to the power $-2/3$.

The PDF $\eta(\psi_m)$ is obtained substituting Eq. (24) into Eq. (16). The ψ_m are generated making use of the rejection method [5]. To apply the rejection method, we use a simplest exponential function as a comparison function f_c:

$$f_c(\psi_m) = \frac{1}{A_0} \exp\left(-\frac{\psi_m}{\psi_0} \right), \quad A_0 = \int_0^\infty \mathrm{d}z C_n^2(z), \quad \psi_0 = 1050 \text{ m}. \tag{25}$$

The simulation results are compared to the theoretical ones in Fig. 2. One can see the same good agreement between the theory and simulation as that for the horizontal path.

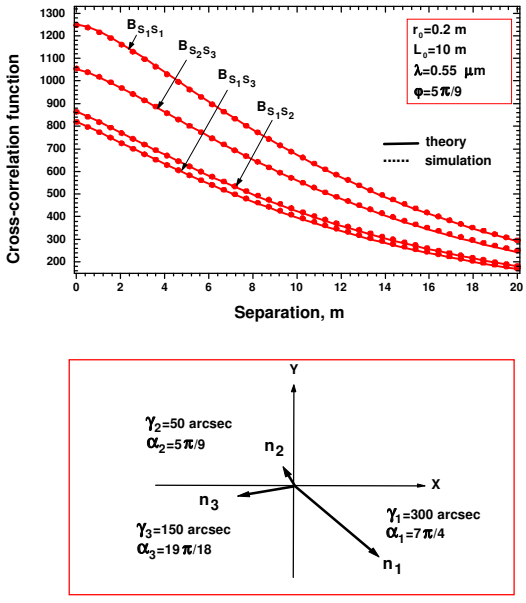

Fig. 2. Theoretical and simulated cross-correlation functions: varying C_n^2 along the path. The description of graph parameters is given in the caption of Fig. 1.

5 Summary

The RWV method has been modified to be suitable for simulation of the phase fluctuations to be produced by many stars. It has turned out that for the special case of weak-turbulence conditions which is of importance for many applications, it is possible to develop a relatively simple and fast procedure of simulations. The validity of theoretical derivations has been verified in the simulation

with both the constant and the varying C_n^2. The comparison of theoretical and simulated results shows that the approach developed reproduces all the needed cross-correlations. The good agreement among the simulated and theoretical results which takes place even for big separations allows for a conclusion about a wide range of possible applications of the approach suggested. Among them are adaptive optics, speckle interferometry, guide stars, long-base interferometry, imaging through the turbulence as well as the simulations of the turbulence-degraded images of extended objects.

6 Acknowledgments

This work was supported by Consejo Nacional de Ciencia y Tecnologia (Mexico) project 1020P-E9507 and by Sistema Nacional de Investigadores (Mexico).

References

[1] D. Kouznetsov, V. V. Voitsekhovich, and R. Ortega-Martinez, "Simulation of turbulence-induced phase and log-amplitude distortions," Appl. Opt. **36**, 464-469 (1997).

[2] V. V. Voitsekhovich, D. Kouznetsov, V. G. Orlov, and S. Cuevas, "Method of random wave vectors in simulation of anisoplanatic effects", ESO/OSA Topical Meetings on Astronomy with Adaptive Optics, 1998.

[3] V. I. Tatarski, *The Effects of the Turbulent Atmosphere on Wave Propagation* (National Science Foundation Report TT-68-50464, 1968).

[4] G. W. Reinhardt, and S .A. Collins, "Outer scale effects in turbulence-degraded light-beam spectra," J. Opt. Soc. Am. **62,** 1526-1528 (1972).

[5] W. H. Press, B. P. Flannery, S. A. Teukolsky, and W. T. Vetterling, *Numerical Recipes in C,* Second Edition, Ch. 7 (Cambridge University Press, Cambridge, 1995).

[6] F. Roddier, "The effects of atmospheric turbulence in optical astronomy," In. *Progress in Optics,* v. **19**, 281-376 (1981).

[7] R. E. Hufnagel, "Variation of atmospheric turbulence," in *Optical Propagation through Turbulence*, OSA Technical Digest Series (OSA, Washington, D.C., 1974), p.WA1-1 – WA1-4.